

SUPPORTING INFORMATION

Nanophase-Photocatalysis: Loading, Storing, and Release of H<sub>2</sub>O<sub>2</sub> using Graphitic Carbon Nitride

Akalya Karunakaran <sup>a,b</sup>, Katie J. Francis <sup>a</sup>, Chris R. Bowen <sup>b</sup>, Richard J. Ball <sup>c</sup>, Yuanzhu Zhao <sup>a</sup>, Lina Wang <sup>a</sup>, Neil B. McKeown <sup>d</sup>, Mariolino Carta <sup>e</sup>, Philip J. Fletcher <sup>f</sup>, Remi Castaing <sup>f</sup>, Mark A. Isaacs <sup>g</sup>, Laurence J. Hardwick <sup>h,i</sup>, Gema Cabello <sup>h,j</sup>, Igor V. Sazanovich <sup>k</sup>, Frank Marken <sup>\*a</sup>

Content

Experimental ..... 1  
X-ray photoelectron spectroscopy (XPS) analysis ..... 2  
Raman analysis ..... 5  
Thermogravimetric analysis ..... 6

Experimental

Materials. Melamine (>99% purity) was obtained from Sigma-Aldrich. PIM-1 was synthesised following a literature procedure.<sup>1,2</sup> Isopropanol and DMSO (both >99% purity) were obtained from Sigma-Aldrich. Para-nitrophenol was purchased from Sigma-Aldrich.

Procedures. Synthesis of g-C<sub>3</sub>N<sub>4</sub>: 5 g of melamine is placed into a ceramic boat with a loose lid and then placed into a tube furnace. The temperature was quickly ramped up to 500 °C and left for 4 h.

After cooling down to room temperature, the yellow product (see Fig. S1, g-C<sub>3</sub>N<sub>4</sub>) was powdered and kept in a glass vial in the dark.

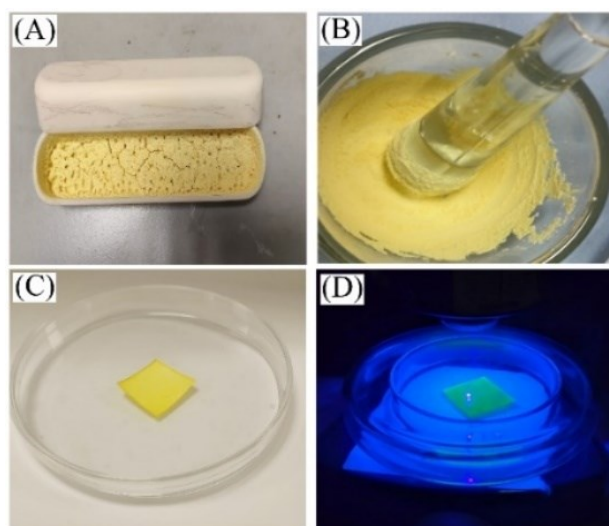


Figure S1. Photographs of (A) furnace boat with freshly formed g-C<sub>3</sub>N<sub>4</sub>, (B) ground g-C<sub>3</sub>N<sub>4</sub>, (C) g-C<sub>3</sub>N<sub>4</sub>@PIM-1 (5:1 weight ratio) in a Petri dish, and (D) exposed to blue light and isopropanol vapour.

<sup>a</sup> Department of Chemistry, University of Bath, Claverton Down, Bath BA2 7AY, UK

<sup>b</sup> Department of Mechanical Engineering, University of Bath, Claverton Down, Bath BA2 7AY, UK

<sup>c</sup> Department of Architecture & Civil Engineering, University of Bath, Claverton Down, Bath BA2 7AY, UK

<sup>d</sup> EaStCHEM School of Chemistry, University of Edinburgh, Joseph Black Building, David Brewster Road, Edinburgh, Scotland EH9 3JF, UK

<sup>e</sup> Department of Chemistry, Swansea University, College of Science, Grove Building, Singleton Park, Swansea SA2 8PP, UK

<sup>f</sup> University of Bath, Materials & Chemical Characterisation Facility, MC2,

<sup>g</sup> HarwellXPS, Research Complex at Harwell, STFC Rutherford Appleton Laboratory, Harwell Campus, Didcot, OX11 0FA, UK

<sup>h</sup> Stephenson Institute for Renewable Energy, Department of Chemistry, University of Liverpool, Liverpool L69 7ZF, UK

<sup>i</sup> The Faraday Institution, Harwell Campus, Didcot, OX11 0RA, UK

<sup>j</sup> Schlumberger Cambridge Research, High Cross, Madingley Road, Cambridge CB3 0EL, UK

<sup>k</sup> Central Laser Facility, Research Complex at Harwell, STFC Rutherford Appleton Laboratory, Harwell Campus, Didcot OX11 0QX, UK

The g-C<sub>3</sub>N<sub>4</sub>@PIM-1 composite films was obtained by a drop casting method. 5 mg of graphitic carbon nitride particles are added to solution containing 1 mg of PIM-1 in 1 cm<sup>3</sup> chloroform and sonicated for 15 minutes. Then, a small amount of the solution is drop cast onto a filter paper with a size 2 x 2cm<sup>2</sup> (WHATMAN with pore size < 2 μm), allowed to dry, and the process is repeated until the entire amount has been deposited.

The photochemical reaction was performed by placing the g-C<sub>3</sub>N<sub>4</sub> powder or g-C<sub>3</sub>N<sub>4</sub>@PIM-1 in a Petri dish. Then, the sample was exposed to the blue light (Thorlabs M385LP1 with typically 80 mW cm<sup>-2</sup> 385 nm light in approx. 2 cm distance, 30 minutes) in the presence of isopropanol vapour (see Fig. S1(D)).

## CHEMICAL COMMUNICATIONS

The detection of hydrogen peroxide ( $\text{H}_2\text{O}_2$ ) was performed by reaction with *para*-nitrophenol and LC/MS detection.<sup>3</sup> Briefly, a mass of 5 mg of  $\text{g-C}_3\text{N}_4$  or  $\text{g-C}_3\text{N}_4@\text{PIM-1}$  was added to 1  $\text{cm}^3$  deionized water. After 5 minutes the sample solution was filtered with 0.2  $\mu\text{m}$  filter. The hydrogen peroxide concentration produced by the catalyst was quantified via an indirect method. Quantifying the amount of *para*-nitrophenol provided the concentration of hydrogen peroxide. The mechanism is based on the reaction of 4-nitrophenyl boronic acid to *para*-nitrophenol. Briefly, hydrogen peroxide reacts with 4-nitrophenyl boronic acid to give *para*-nitrophenol. For detection a reagent 100  $\mu\text{L}$  prepared 1:1 DMSO and 4-nitrophenyl boronic acid was added to 10  $\text{cm}^3$  solution (10% dimethyl sulfoxide and 90% of 0.1 M carbonate buffer solution with  $\text{pH}=9$ ). A 1  $\text{cm}^3$  reagent solution was added to the  $\text{g-C}_3\text{N}_4$  sample solution in the absence of light and left for approx. 60 minutes to react. The experiment was carried out in absence of light as much as possible. The resultant solution was diluted to a ratio of 1/50 with 90% deionized water and 10% DMSO, which stopped the reaction. Detection was then achieved with mass spectrometry with an Automated Agilent QTOF (Walkup) used with HPLC (four chromatography columns) and a variable wavelength detector (VWD).

## X-ray photoelectron spectroscopy (XPS) analysis

XPS data was acquired using a Kratos Axis SUPRA using monochromated Al  $\text{K}\alpha$  (1486.69 eV) X-rays at 15 mA emission and 12 kV HT (180W) and a spot size/analysis area of 700 x 300  $\mu\text{m}$ . The instrument was calibrated to gold metal Au 4f (83.95 eV) and dispersion adjusted give a BE of 932.6 eV for the Cu 2p<sub>3/2</sub> line of metallic copper. Ag 3d<sub>5/2</sub> line FWHM at 10 eV pass energy was 0.544 eV. Source resolution for monochromatic Al  $\text{K}\alpha$  X-rays was  $\sim 0.3$  eV. The instrumental resolution was determined to be 0.29 eV at 10 eV pass energy using the Fermi edge of the valence band for metallic silver. Resolution with charge compensation system on  $<1.33$  eV FWHM on PTFE. High resolution spectra were obtained using a pass energy of 20 eV, step size of 0.1 eV and sweep time of 60s, resulting in a line width of 0.696 eV for Au 4f<sub>7/2</sub>. Survey spectra were obtained using a pass energy of 160 eV. Charge neutralisation was achieved using an electron flood gun with filament current = 0.4 A, charge balance = 2 V, filament bias = 4.2 V. Successful neutralisation was adjudged by analysing the C 1s region wherein a sharp peak with no lower BE structure was obtained. Spectra have been charge corrected to the main line of the carbon 1s spectrum (adventitious carbon) set to 284.8 eV. All data was recorded at a base pressure of below  $9 \times 10^{-9}$  Torr and a room temperature of 294 K. Data was analysed using CasaXPS v2.3.19PR1.0. Peaks were fit with a Shirley background prior to component analysis.

XPS data were obtained first at  $-110$  °C and then at ambient temperature to explore evaporative losses under high vacuum conditions. For the untreated sample C1s, N1s, and O1s signals were, which is observed consistent with previously reported data.<sup>4</sup>

Spectral deconvolution via non-linear least squares fitting determined the presence of CNC (398.7 eV),  $\text{N}_3\text{C}$  (399.9 eV) and CNH (401.1 eV) in the N 1s region, and C=N (288.3 eV), C-O/C-N (286 eV) and CC/CH (284.8 eV) as expected for graphitic carbon nitride.

One peak in O1s (532.0 eV) with broader FWHM could contain both C-O and C=O. Upon warming the sample to ambient temperature, the main features remain, although the O1s signal is lower in intensity. An additional feature at high binding energy can be seen in both the C 1s and N 1s regions, due to a shake-up feature from  $\pi\text{-}\pi^*$  interactions.

XPS data for the blue light and isopropanol vapour treated  $\text{g-C}_3\text{N}_4$  shows similar N1s, C1s, and O1s features with a higher O1s signal in particular at lower temperature. The ratio of C-C (279.6 eV) to C-N=C (282.9 eV) at the surface seem to be increased, which could be linked to some isopropanol bound to the surface.

Comparing light treated and untreated  $\text{g-C}_3\text{N}_4$  XPS data (Table S3,4 with Table S1,2) it is clear that light treatment increases the C-O/C=O atomic % (2.4 and 1.2 to 5.3 and 4.2 at% at low T and RT respectively) and CC/CH peaks (3.2 and 1.9 to 18.5 and 12.5 at% respectively), with corresponding decreases to the CNC and C=N XPS At%. This is evidence for surface changes due to the photochemical process within the  $\text{g-C}_3\text{N}_4$ . This shift to C-O functionalities could be linked to bound reaction products (*e.g.* acetone and peroxides).

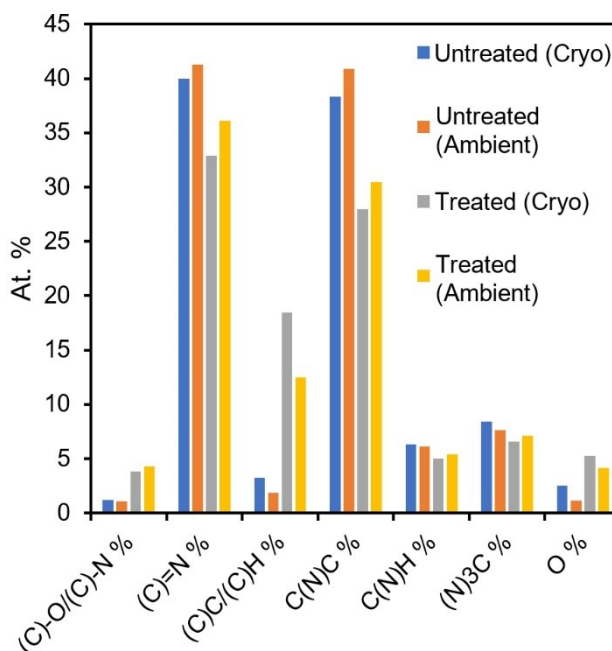


Figure S2. Compositional quantifications from XPS analysis

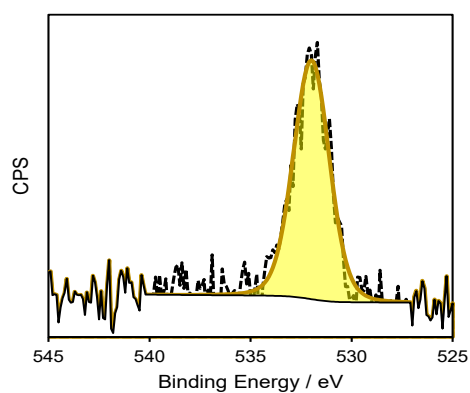
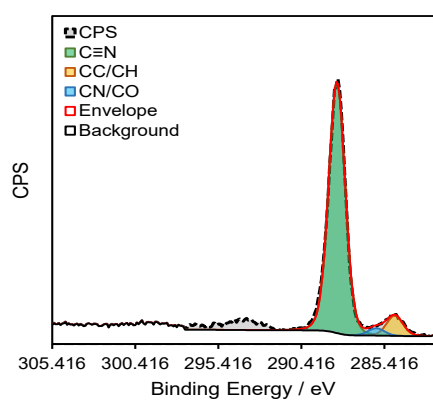
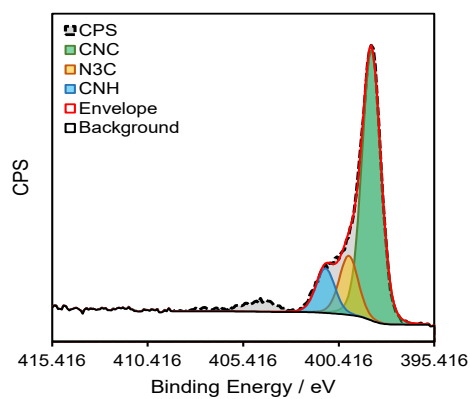
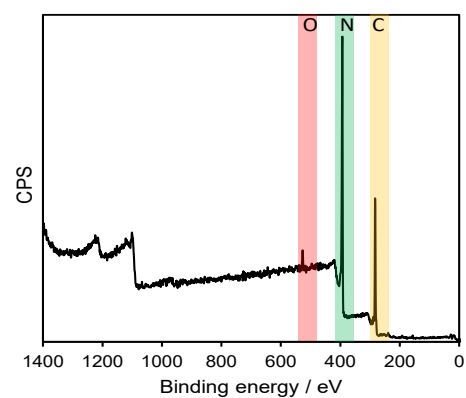


Figure S3. XPS survey spectra of untreated  $g\text{-C}_3\text{N}_4$  with data plots for N1s, C1s, and O1s, at cryo temperature.

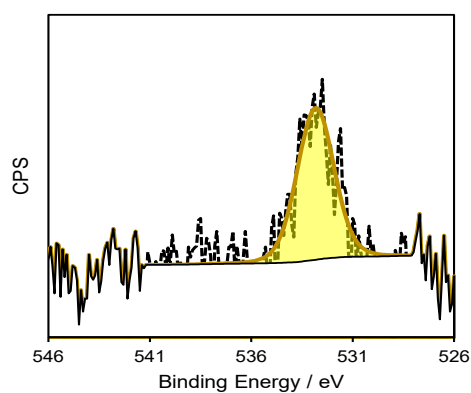
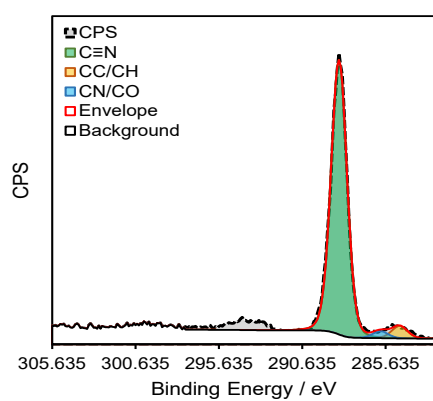
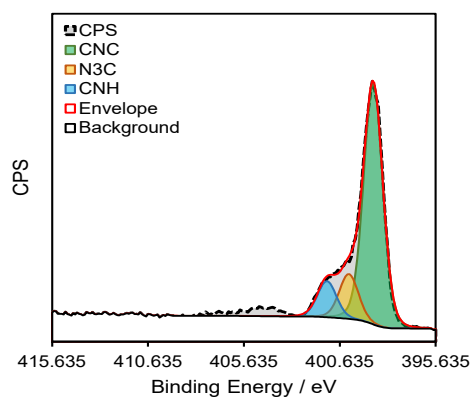
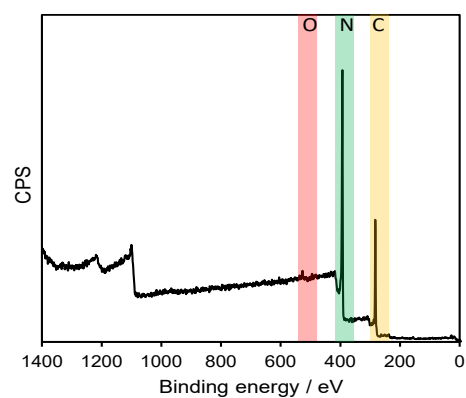


Figure S4. XPS survey spectra of untreated  $g\text{-C}_3\text{N}_4$  with data plots for N1s, C1s, and O1s, at ambient temperature.

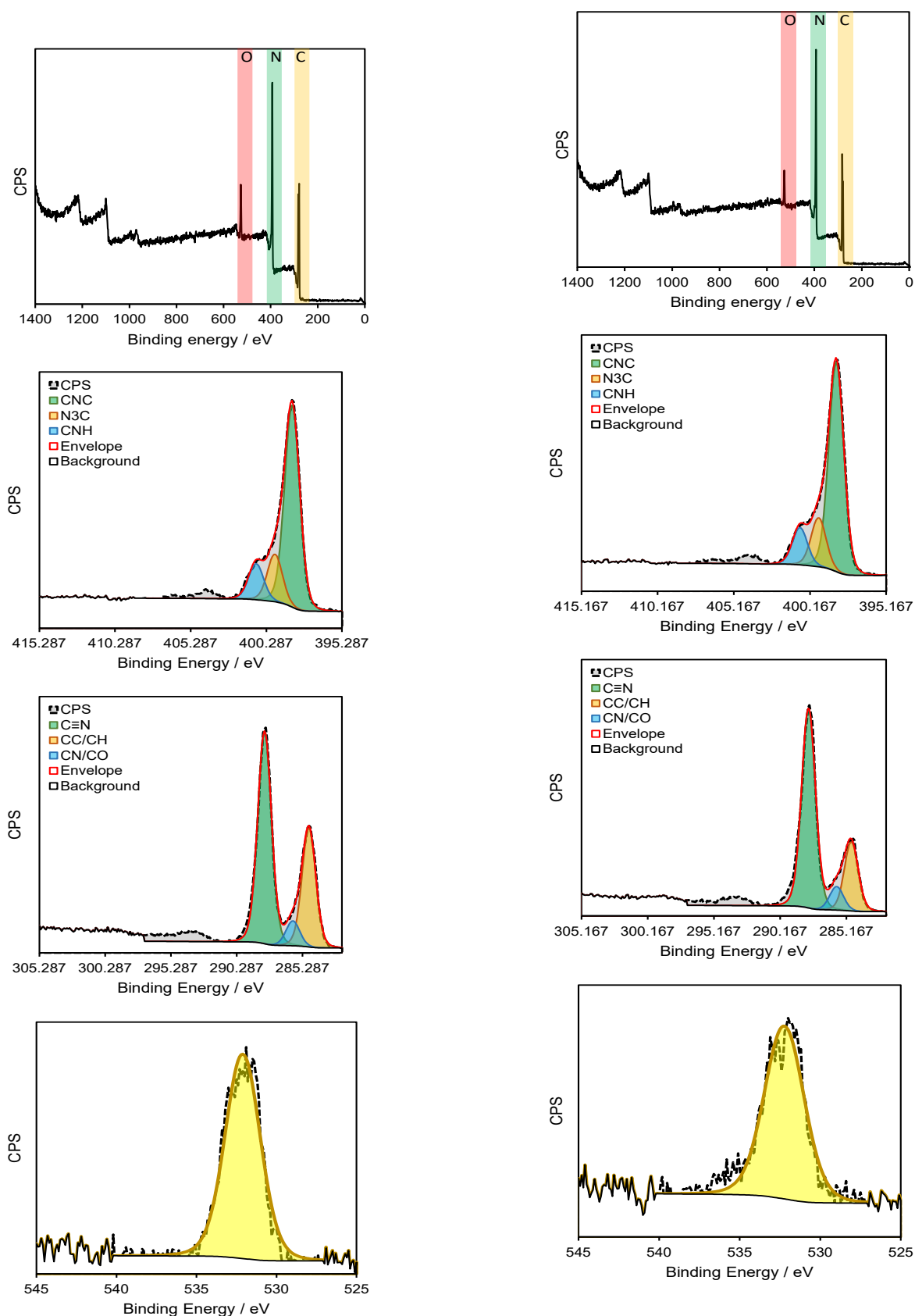


Figure S5. XPS survey spectra of blue light treated  $g\text{-C}_3\text{N}_4$  with data plots for N1s, C1s, and O1s, at cryo temperature.

Figure S6. XPS survey spectra of blue light treated  $g\text{-C}_3\text{N}_4$  with data plots for N1s, C1s, and O1s, at ambient temperature.

Table S1. XPS data analysis for g-C<sub>3</sub>N<sub>4</sub> (untreated, low T).

X	Species	BE / eV	FWHM / eV	Area	At. %
N	CNC	398.7	1.2	5281.4	38.4
	N3C	399.9	1.2	1157.2	8.4
	CNH	401.1	1.2	870.6	6.3
C	C=N	288.3	1.2	2949.7	40.0
	CC/CH	284.8	1.2	237.6	3.2
	C-O/C-N	285.9	1.2	86.6	1.2
O	C-O/C=O	532.4	2.1	599.1	2.5

Table S4. XPS data analysis for g-C<sub>3</sub>N<sub>4</sub> (light treated, ambient T).

X	Species	BE / eV	FWHM / eV	Area	At. %
N	CNC	398.4	1.2	4202.7	30.5
	N3C	399.6	1.2	982.9	7.1
	CNH	400.8	1.2	749.0	5.4
C	C=N	288.0	1.2	2666.1	36.1
	CC/CH	284.8	1.2	922.9	12.5
	C-O/C-N	285.9	1.2	314.4	4.3
O	C-O/C=O	532.4	2.9	992.5	4.2

Table S2. XPS data analysis for g-C<sub>3</sub>N<sub>4</sub> (untreated, ambient T).

X	Species	BE / eV	FWHM / eV	Area	At. %
N	CNC	398.9	1.2	5712.4	40.9
	N3C	400.2	1.2	1062.2	7.6
	CNH	401.3	1.2	855.0	6.1
C	C=N	288.4	1.1	3086.3	41.3
	CC/CH	284.8	1.1	139.7	1.9
	C-O/C-N	286.0	1.1	78.0	1.0
O	C-O/C=O	532.5	2.1	277.2	1.2

Table S3. XPS data analysis for g-C<sub>3</sub>N<sub>4</sub> (light treated, low T).

X	Species	BE / eV	FWHM / eV	Area	At. %
N	CNC	398.6	1.2	3587.5	27.9
	N3C	399.7	1.2	846.5	6.6
	CNH	401.0	1.2	641.1	5.0
C	C=N	288.2	1.2	2262.7	32.9
	CC/CH	284.8	1.2	1267.6	18.5
	C-O/C-N	286.0	1.2	265.2	3.9
O	C-O/C=O	532.4	2.6	1161.9	5.3

## Raman analysis

Raman data for solid powder samples were obtained with a Raman spectrometer/microscope (wavelength 785 nm excitation; with a Renishaw inVia confocal Raman microscope, 1% power, severe fluorescence was observed especially at shorter excitation wavelengths, background was subtracted). The main peaks/features are consistent with literature data for similar materials.<sup>5</sup> When comparing the g-C<sub>3</sub>N<sub>4</sub> before and after blue light/isopropanol vapour treatment, there are no significant changes.

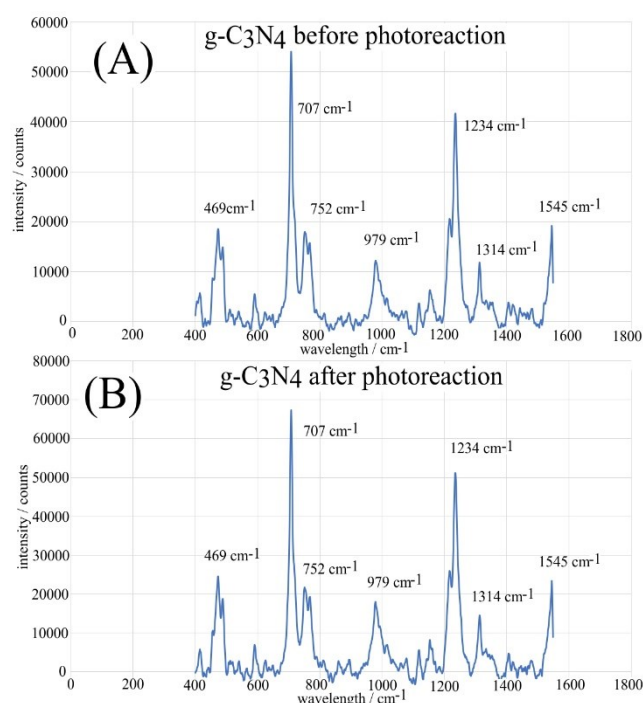


Figure S7. Raman spectra (785 nm) for powder samples (A) before and (B) after blue light/isopropanol vapour treatment.

## CHEMICAL COMMUNICATIONS

In order to further explore any surface bound peroxo-species whilst suppressing fluorescence background, Kerr-gated Raman spectra were acquired at ULTRA laser facilities (Central Laser Facility, STFC, Rutherford Appleton Laboratories).<sup>6,7,8</sup> Spectra were collected under 633 nm laser pulse (3 mW, 10 kHz, 2 ps) with a 75 x 75  $\mu\text{m}^2$  spot size. The Kerr-gate was activated by a gating pulse (800 nm, 240  $\mu\text{J}$ , 2 ps, 10 kHz). All spectra were collected and averaged over 5 repeats, each with an acquisition time of 60 s and slit size 300  $\mu\text{m}$ . The Raman shift was calibrated against the spectrum obtained for toluene.

Au nanoparticles (AuNPs) of 55 nm average diameter were employed to achieve surface enhancement of Raman spectroscopy. Au nanoparticles were synthesized by chemical reduction of  $\text{HAuCl}_4 \cdot 3\text{H}_2\text{O}$  with sodium citrate, following the Turkevich-Frens method.<sup>9,10</sup>

All data traces (Fig. S8) suggest that there are no distinct peroxo-species present (expected and a previously observed<sup>11</sup> band at ca. 891  $\text{cm}^{-1}$ ) bound to the sample surface (for both solid and solution phase) at a concentration that would be detectable.

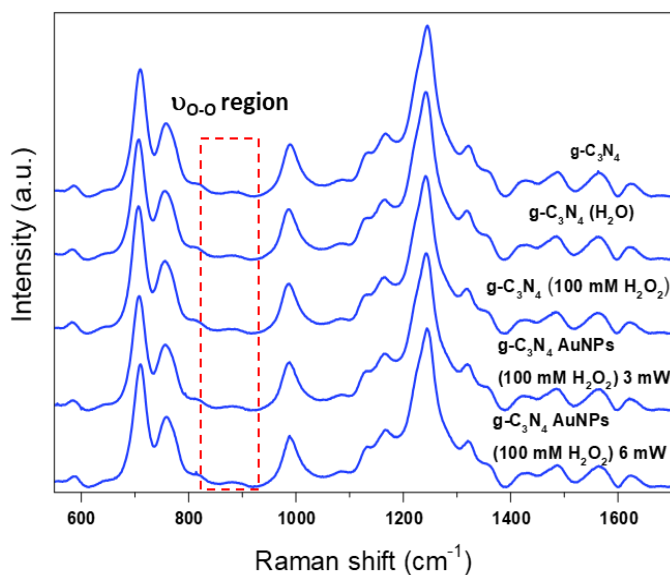


**Figure S8.** Kerr gated Raman (3 mW power) data for  $\text{g-C}_3\text{N}_4$  (a);  $\text{g-C}_3\text{N}_4$  in  $\text{H}_2\text{O}$  (b);  $\text{g-C}_3\text{N}_4$  in 100 mM  $\text{H}_2\text{O}_2$  (c);  $\text{g-C}_3\text{N}_4$  with a layer of AuNPs, in 100 mM  $\text{H}_2\text{O}_2$  (d);  $\text{g-C}_3\text{N}_4$  with a layer of AuNPs, in 100 mM  $\text{H}_2\text{O}_2$  and 6 mW laser power (e). All data obtained under 633 nm excitation line.

### Thermogravimetric analysis

In order to verify and quantify the presence of water bound in  $\text{g-C}_3\text{N}_4$ , TGA experiments were performed for both pure  $\text{g-C}_3\text{N}_4$  and  $\text{g-C}_3\text{N}_4$  after blue light/isopropanol vapour treatment. Both measurements clearly verified bound water (approx 2.5 wt% before and approx 2.7 wt% after blue light/isopropanol treatment) suggesting typically one water molecule for 3-4 heptazine units or the presence of ambient nanophase water within  $\text{g-C}_3\text{N}_4$ .

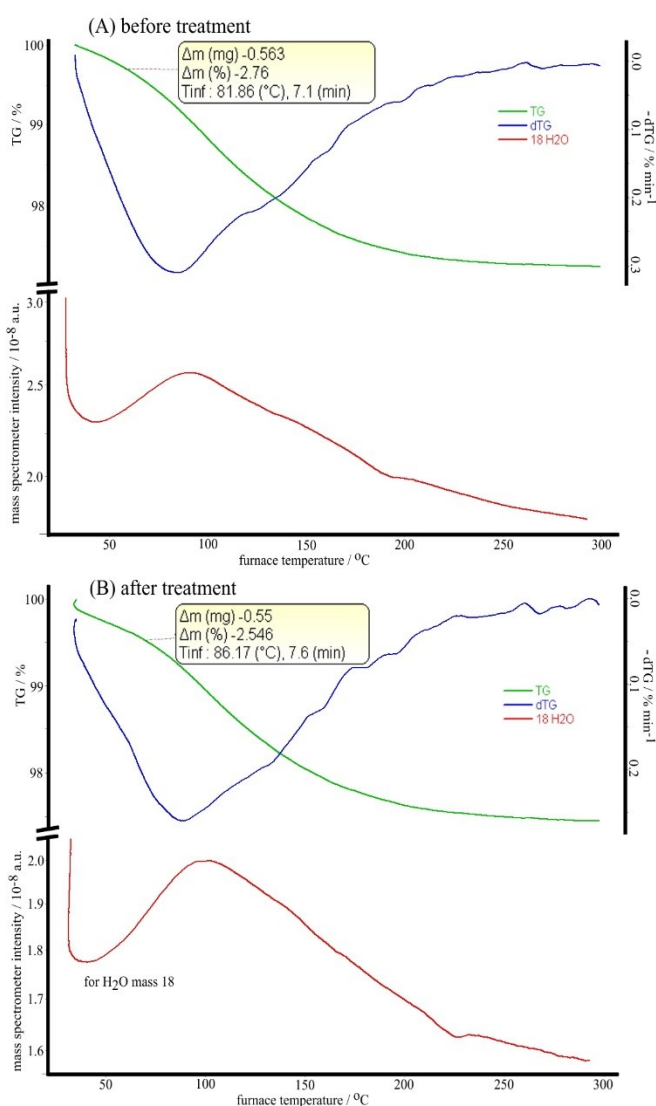


**Figure S9.** Thermogravimetric analysis (TGA) for (A)  $\text{g-C}_3\text{N}_4$  before and (B) after blue light/isopropanol vapour treatment. Shown are (i) the thermogravimetry trace (TG), (ii) the derivative of the thermogravimetry (dTG), and (iii) the mass spectrometric detection of water with mass 18  $\text{g mol}^{-1}$ .

Evolving gases were sent through a stainless-steel capillary to a Pfeiffer Vacuum Omnistar GSD 320 mass spectrometer, equipped with a quadrupole mass analyser and a SEM detector. The mass spectrometry data (simultaneously recorded) confirm the loss of water in the temperature range from 50  $^{\circ}\text{C}$  to 200  $^{\circ}\text{C}$ . A slight mismatch in peak position comparing differential thermogravimetry trace and mass spectrometry trace is due to a signal delay in the mass spectrometer.

## CHEMICAL COMMUNICATIONS

- 1 P.M. Budd, E.S. Elabas, B.S. Ghanem, S. Makhseed, N.B. McKeown, K.J. Msayib, C.E. Tattershall and D. Wang, *Adv. Mater.* 2004, **16**, 456–457.
- 2 P.M. Budd, B.S. Ghanem, S. Makhseed, N.B. McKeown, K.J. Msayib and C.E. Tattershall, *Chem. Commun.* 2004, 230–231.
- 3 L.A. Wang, M. Carta, R. Malpass-Evans, N.B. McKeown, P.J. Fletcher, P. Estrela, A. Roldan and F. Marken, *J. Catal.* 2022, **416**, 253–266.
- 4 Y.Z. Zhao, L.N. Wang, R. Malpass-Evans, N.B. McKeown, M. Carta, J.P. Lowe, C.L. Lyall, R. Castaing, P.J. Fletcher, G. Kociok-Kohn, J. Wenk, Z.Y. Guo and F. Marken, *ACS Appl. Mater. Interfaces* 2022, **14** (17), 19938–19948.
- 5 P.V. Zinin, L.C. Ming, S.K. Sharma, V.N. Khabashesku, X.R. Liu, S.M. Hong, S. Endo and T. Acosta, *Chem. Phys. Lett.* 2009, **472** (1-3), 69–73.
- 6 I.V. Sazanovich, G.M. Greetham, B.C. Coles, I.P. Clark, P. Matousek, A.W. Parker and M. Towrie, Facility development update: the Kerr-gated Raman/ultrafast time-resolved fluorescence instrument. *Cent. Laser Facil. Annu. Rep.*, 2014–2015, 44.
- 7 L. Cabo-Fernandez, A.R. Neale, F. Braga, I.V. Sazanovich, R. Kosteckic and L.J. Hardwick, *Phys. Chem. Chem. Phys.* 2019, **21**, 23833–23842.
- 8 A.R. Neale, D.C. Milan, F. Braga, I.V. Sazanovich, and L.J. Hardwick, *ACS Energy Lett.* 2022, **7** (8), 2611–2618.
- 9 J. Turkevich, P. Stevenson and J. Hillier, *Disc. Faraday Soc.*, 1951, **11**, 55–75.
- 10 G. Frens, *Nat. Phys. Sci.* 1973, **241**, 20–22.
- 11 Y. Shiraishi, S. Kanazawa, Y. Sugano, D. Tsukamoto, H. Sakamoto, S. Ichikawa, T. Hirai, *ACS Catal.* 2014, **4**, 774–780.